Single beam acoustic trapping

Jungwoo Lee,[1,a)] Shia-Yen Teh,[2] Abraham Lee,[2] Hyung Ham Kim,[1] Changyang Lee,[1] and K. Kirk Shung[1]
[1]*Department of Biomedical Engineering, University of Southern California, Los Angeles, California 90089, USA*
[2]*Department of Biomedical Engineering, University of California at Irvine, Irvine, California 92697, USA*

(Received 2 June 2009; accepted 21 July 2009; published online 17 August 2009)

A single beam acoustic device, with its relatively simple scheme and low intensity, can trap a single lipid droplet in a manner similar to optical tweezers. Forces in the order of hundreds of nanonewtons direct the droplet toward the beam focus, within the range of hundreds of micrometers. This trapping method, therefore, can be a useful tool for particle manipulation in areas where larger particles or forces are involved. © *2009 American Institute of Physics*. [DOI: 10.1063/1.3206910]

Optical trapping of small objects has been used to quantitatively investigate the mechanism of biological particles.[1,2] Optical tweezers[3] typically output forces on the order of piconewtons, and displace micrometer-sized particles up to hundreds of nanometers from the trap. Despite its precision and wide range of biological applications, however, its use has been limited to either optically purified samples or shallow regions in a medium. The high energy of focused lasers, in addition, has often induced photodamage on target particles.[4]

In acoustics, Wu[5] introduced the term of acoustic tweezers and showed that latex spheres or clusters of frog eggs could be trapped by applying two opposing sound waves at 3.5 MHz. Here we present a single beam acoustic trapping that is similar to optical tweezers and differs from Wu's[5] dual beam method, based on our theoretical findings in ray acoustics regime: the tight focusing, the acoustic impedance match of particles with surrounding medium, and the particle size greater than the ultrasonic wavelength.[6–8] Note that only the transverse trapping was demonstrated in the present experiment because an axial focusing as tight as the lateral focusing could not be achieved.

A 30 MHz lithium niobate ($LiNbO_3$) single element transducer was built to trap lipid droplets and driven by sinusoidal bursts. Note that the transducer was allowed to move only in the direction perpendicular to the beam axis [see Fig. 1(a)]. The excitation frequency was varied from 23 to 37 MHz, and its peak-to-peak voltages were 22, 32, and 41 V_{pp}. Due to the need for sharp intensity gradients, the transducer was press focused[9] to obtain an F-number of 0.75. The transducer was mounted on a three-dimensional motorized positioner (LMG26 T50MM, OptoSigma, USA), and a series of control commands was sent to the positioner by the customized LABVIEW controller [see Fig. 1(b)]. To evaluate generated forces by the transducer, the acoustic peak pressures at different frequencies were measured at the focus, by a calibrated PVDF needle hydrophone having an active element size of 40 μm (HPM04/01, Precision Acoustics, U.K.), as shown in Fig. 2(a).

Oleic acid lipid droplets of 126.0 ± 5.6 μm in diameter were synthesized using droplet-based microfluidic devices, a robust method of forming monodispersed droplets in the nanometer to micrometer size range.[10] A single droplet was used as a target particle because of its good acoustic impedance match with the de-ionized water. The droplets were then carefully loaded underneath an acoustically transparent mylar film in the water chamber. The film acted against the buoyancy of lipid droplets, while maintaining those droplets within the field of view of the microscope. It should be noted here that a majority of optical tweezer experiments has also been carried out in this manner. The distance between the transducer and the film remained at 3 mm.

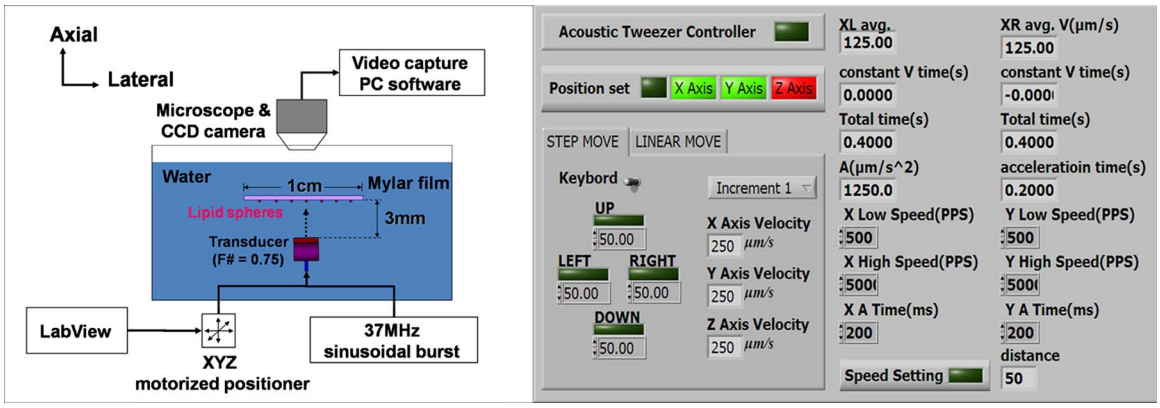

FIG. 1. (Color online) (a) (left) Experimental configuration of acoustic traps. (b) (right) LABVIEW interface for three dimensional linear stepping motions.

[a)]Author to whom correspondence should be addressed. Electronic mail: jungwool@usc.edu.

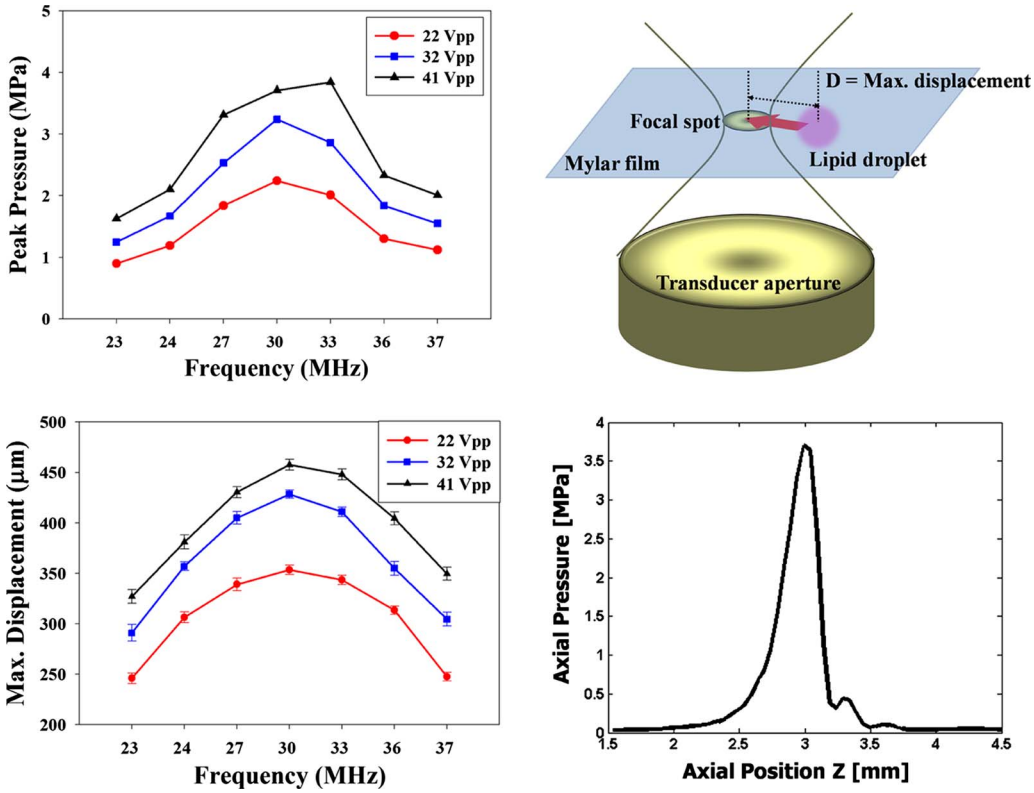

FIG. 2. (Color online) (a) (upper left) Peak pressures from 23 to 37 MHz with different excitation voltages at the focus. (b) (upper right) Illustration of maximum displacement measurement. The droplet (a shaded pink circle) was drawn into the focal spot (a shaded gold area) when trapped. (c) (lower left) Maximum displacements as a function of frequency and excitation voltage. (d) (lower right) Axial pressure distribution when V_{pp}=41 V at 30 MHz.

The maximum displacement D was defined, as in Fig. 2(b), and then measured to indicate how far the trapping can attract the droplet from the center of the trap [see Fig. 2(c)]. As shown in Figs. 2(a), 2(c), and 2(d), both maximum displacement and peak pressure were observed at 30 MHz. In general, the higher excitation voltages induced the longer displacements. For example, at 30 MHz, the average maximum displacement of the trapped droplet was 428.5 μm with 32 V_{pp}, whereas it was 353.5 μm with 22 V_{pp}. The broad bandwidth of the transducer made it possible to capture droplets of different sizes (see Fig. 3) since the particle size that can be trapped depends on the driving frequency. This trapping scheme thus demonstrates that a particle of a certain size might be trapped and yet separated from others by choosing the proper frequency. Owing to the tight focusing, the 3 dB pressure gradient was measured as 52.6 MPa/mm, at 30 MHz and 32 V_{pp}, as compared with 35.5 MPa/mm when the input voltage was decreased to 22 V_{pp}. Note that the gradient was 0.13 MPa/mm in Wu's[5] method.

FIG. 3. (Color online) Trapped droplet motion I (enhanced online). [URL: http://dx.doi.org/10.1063/1.3206910.1]

The maximum trapping forces in the transverse direction were calculated by

$$F_y = \frac{P}{\pi c_w}\int_0^{2\pi}\int_{\theta_{\min}}^{\theta_{\max}}\left(\frac{r}{w(z)}\right)^2 \exp\left[\frac{-2(x^2+y^2)}{w(z)^2}\right]\frac{\cos\theta_i}{R_A} \times\left\{\left(Q_s+\frac{Q_g}{\tan\alpha}\right)y_A - \frac{R_A Q_g}{L_B \sin\alpha} y_C\right\}\sin\theta d\theta d\varphi, \quad (1)$$

$$Q_s = 1 + R\cos 2\theta_i - \frac{T^2[\cos(2\theta_i - 2\theta_r) + R\cos 2\theta_i]}{1 + R^2 + 2R\cos 2\theta_r}, \quad (2)$$

$$Q_g = R\sin 2\theta_i - \frac{T^2[\sin(2\theta_i - 2\theta_r) + R\sin 2\theta_i]}{1 + R^2 + 2R\cos 2\theta_r}. \quad (3)$$

The parameters used in the above expressions are defined in Fig. 4. For example, the estimated forces at 30 MHz were 125 and 247 nN when driven by 22 and 32 V_{pp}, respectively. These results so far indicate that this method may induce not only a wider trapping region but a stronger attractive force toward the trap than its optical counterpart.

The trapped droplet moved with a certain lag, proportional to its distance from the trap. The farther distance resulted in the longer lag. As the droplet left the center of the trap, restoring forces pulled it back to the center (see Fig. 5). Hence the droplet behaved as if attached to the center of the trap by a spring as in optical traps.

The experimental results demonstrated that acoustic traps occur around a tight focus and the resultant forces depend on the droplet size, frequency of the wave, and the

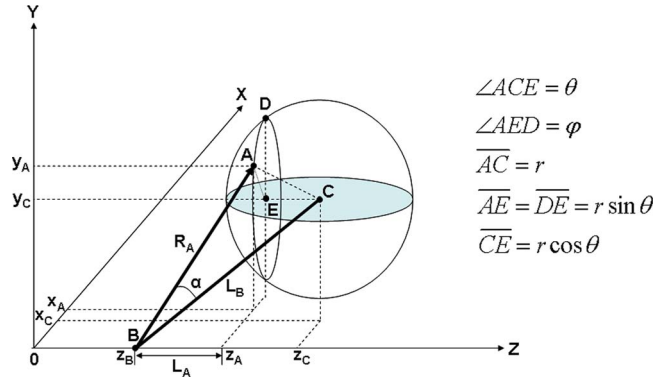

FIG. 4. (Color online) Definition of parameters to calculate the transverse trapping force on a sphere centered at C (x_c, y_c, z_c) (Ref. 7).

excitation energy. The spatial range of the traps was much wider than that of optical traps. By increasing the frequency, it is conceivable that this acoustic device will be capable of manipulating particles much smaller than currently reported. Many potential biomedical applications including measuring intercellular forces, such as those between erythrocytes and sperm motility, are envisioned.

This work has been supported by NIH Grant Nos. R21-EB5202 and P41-EB2182 and Memorial Funds of Professor H. K. Cheng at USC.

FIG. 5. (Color online) Trapped droplet motion II (enhanced online). [URL: http://dx.doi.org/10.1063/1.3206910.2]

[1]M. D. Wang, M. J. Schnitzer, H. Yin, R. Landrick, J. Gelles, and S. M. Block, Science **282**, 902 (1998).
[2]A. D. Mehta, M. Rief, J. A. Spudick, D. A. Smith, and R. H. Simmons, Science **283**, 1689 (1999).
[3]A. Ashkin, J. M. Dziedzic, J. E. Bjorkholm, and S. Chu, Opt. Lett. **11**, 288 (1986).
[4]K. C. Neuman and A. Nagy, Nat. Methods **5**, 491 (2008).
[5]J. Wu, J. Acoust. Soc. Am. **89**, 2140 (1991).
[6]J. Lee, K. Ha, and K. K. Shung, J. Acoust. Soc. Am. **117**, 3273 (2005).
[7]J. Lee and K. K. Shung, J. Acoust. Soc. Am. **120**, 1084 (2006).
[8]J. Lee and K. K. Shung, Ultrasound Med. Biol. **32**, 1575 (2006).
[9]J. M. Cannata, T. A. Ritter, W. Chen, R. H. Silverman, and K. K. Shung, IEEE Trans. Ultrason. Ferroelectr. Freq. Control **50**, 1548 (2003).
[10]S. Y. Teh, R. Lin, L. H. Hung, and A. P. Lee, Lab Chip **8**, 198 (2008).